JMEPEG (2015) 24:2738–2743
DOI: 10.1007/s11665-015-1483-4

©ASM International
1059-9495/$19.00

Microstructure and Properties of Ternary Cu-Ti-Sn Alloy

Xianhui Wang, Chunyu Chen, Tingting Guo, Juntao Zou, and Xiaohong Yang

(Submitted May 23, 2014; in revised form August 21, 2014; published online May 19, 2015)

The effect of Sn addition and heat treatment on the microstructure and properties of Cu-3Ti and Cu-2Ti alloys was studied. The microstructure and phase constituents were characterized by an optical microscope, x-ray diffractometer, and transmission electron microscope, and the electrical conductivity and hardness were determined as well. The results show that the as-cast microstructure of Cu-Ti-Sn alloys consists of α-Cu(Ti,Sn) and primary $CuSn_3Ti_5$ intermetallic compound. $CuSn_3Ti_5$ phase has a hexagonal structure with the lattice parameters $a = 0.81737$ nm, $b = 0.81737$ nm, and $c = 0.55773$ nm. With the increase of aging time, the electrical conductivity progressively increases, while the hardness increases and then decreases. After aging at 450 °C for 8 h, Cu-3Ti-2Sn alloy has an electrical conductivity of 23.1 MS/m and a hardness of 134.5 HV, and the electrical conductivity and hardness of Cu-2Ti-2Sn alloy are 21.5 MS/m and 119.3 HV, respectively. An appropriate aging is beneficial for the precipitation of coherent metastable β′-Cu_4Ti phase, which can strengthen Cu-3Ti-2Sn and Cu-2Ti-2Sn alloys. However, a prolonged aging time results in the decrease of hardness due to the formation of incoherent equilibrium β-Cu_3Ti phase. The presence of $CuSn_3Ti_5$ phase reduces the solute Ti content in the copper matrix and, thus, gives rise to the increase of the electrical conductivity of Cu-Ti-Sn alloys.

Keywords alloys, electronic properties, microstructure, phase transitions, precipitation, transmission electron microscopy

1. Introduction

Age-hardened Cu-base alloys are most widely used in the electrical connection, high-strength springs, electrical contacts, and corrosion- and wear-resistant materials (Ref 1–3). Among these copper alloys, Cu-Be alloy has an excellent combination of electrical conductivity and mechanical properties. Nevertheless, its toxicity brings about environmental hazards during the fabrication process. In addition, poor anti-stress relaxation property at elevated temperatures hinders its applications (Ref 4). Subsequently, it is of significance to seek a new material to replace Cu-Be alloy. Currently, Cu-Ti alloy is regarded as the most potential substitute for age-hardened Cu-Be elastic alloy since its mechanical strength is comparable to that of Cu-Be alloy. However, Cu-Ti alloy has a quite low electrical conductivity due to the presence of solute Ti atoms in the copper matrix (Ref 5–10). Hence, it is necessary to improve the electrical conductivity of Cu-Ti alloy without deteriorating mechanical strength. Up to now, a few attempts have been made to improve the electrical conductivity of binary Cu-Ti alloys by reducing solute Ti atoms in the copper matrix. Semboshi et al. (Ref 11) reported that the electrical conductivity of Cu-1 at.% Ti alloy aged in a hydrogen atmosphere can reach up to 27.84 MS/m, which is increased by 167% compared to that of the same alloy aged in a vacuum. The improved electrical conductivity is ascribed to the precipitation of titanium hydride, which reduces the concentration of Ti in the matrix more efficiently than aging in a vacuum. However, the formation of the brittle TiH_2 phase results in a sharp decrease in the hardness of Cu-1 at.%Ti alloy aged in the hydrogen atmosphere in comparison to the vacuum aging treatment. Konno et al. (Ref 12) revealed that the electrical conductivity of Cu-3 at.%Ti alloy with 4 at.%Al addition is 3.48 MS/m, which is about 6 times larger than that without Al addition, whereas the peak hardness decreases from 280 to 180 HV. Markandeya et al. (Ref 13) found that Cd addition decreases the electrical conductivity of Cu-3Ti alloy though the yield strength and tensile strength increase considerably. Lebreton et al. (Ref 14) studied the microstructural evolution and hardness of Cu-Ti-Sn alloys during aging, and good hardness values were obtained, but the effect of Sn addition on the electrical conductivity of Cu-Ti was unclear, and no data were reported on the electrical conductivity of Cu-Ti-Sn alloy in their work. Subsequently, it is necessary to clarify the effect of Sn addition on the electrical conductivity of Cu-Ti alloy. In the present work, Cu-3Ti-2Sn and Cu-2Ti-2Sn alloys were studied by structural observation and electrical and mechanical measurements. The electrical conductivity was examined as a function of aging time to discuss the relationship between microstructural evolution and electrical conductivity of the Cu-Ti-Sn alloy. The purpose is to get a better understanding of microstructural evolution during aging process and to develop a new alloy with a better combination of strength and electrical conductivity in order to extend their applicability among the electronic engineering fields.

Xianhui Wang, School of Materials Science and Engineering, Xi'an University of Technology, Xi'an 710048, People's Republic of China and Institute for Frontier Materials, Deakin University, Waurn Ponds Campus, Victoria 3220, Australia; **Chunyu Chen**, **Juntao Zou**, and **Xiaohong Yang**, School of Materials Science and Engineering, Xi'an University of Technology, Xi'an 710048, People's Republic of China and **Tingting Guo**, Institute for Frontier Materials, Deakin University, Waurn Ponds Campus, Victoria 3220, Australia. Contact e-mail: xhwang693@xaut.edu.cn.

2. Experimental

Button ingots with a nominal composition of Cu-3Ti-2Sn and Cu-2Ti-2Sn alloys were prepared from 99.9% electrolytic copper, 99.9% titanium, and 99.999% tin by arc-melting in a non-consumable vacuum furnace. Each ingot was melted at least four times to guarantee its homogeneity. The ingots were cut into blocks, which were subsequently solution-treated at 800 °C for 4 h, followed by water quenching. Finally, the aging treatments were performed in a furnace under an argon atmosphere at 450 °C for 0.5, 1, 4, and 8 h, respectively. Electrical conductivity was measured by a 7501A eddy current gage. Vickers hardness (HV) test was performed on a

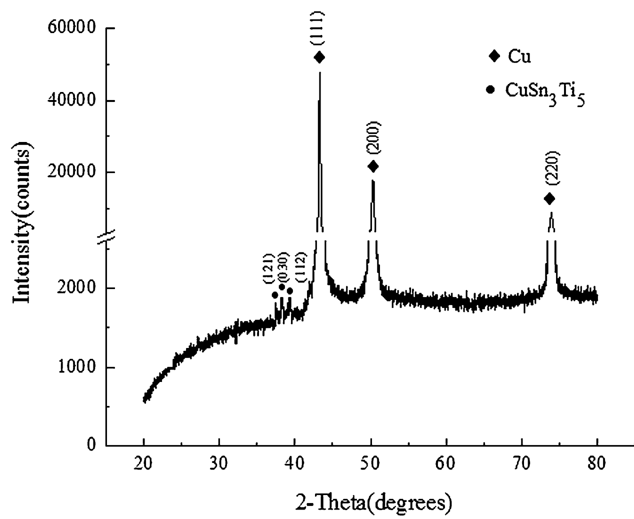

Fig. 1 XRD pattern of the as-cast Cu-3Ti-2Sn alloy

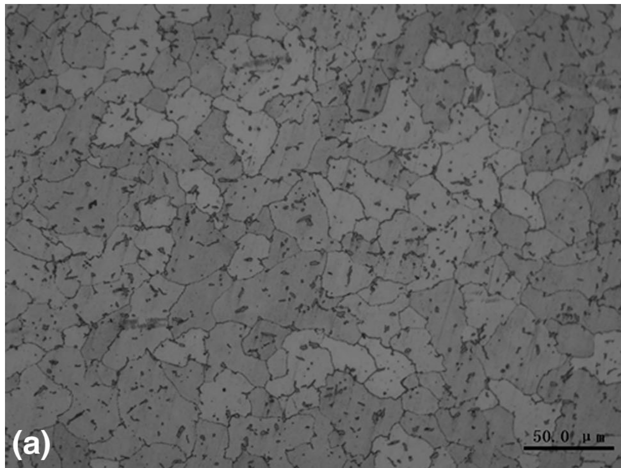

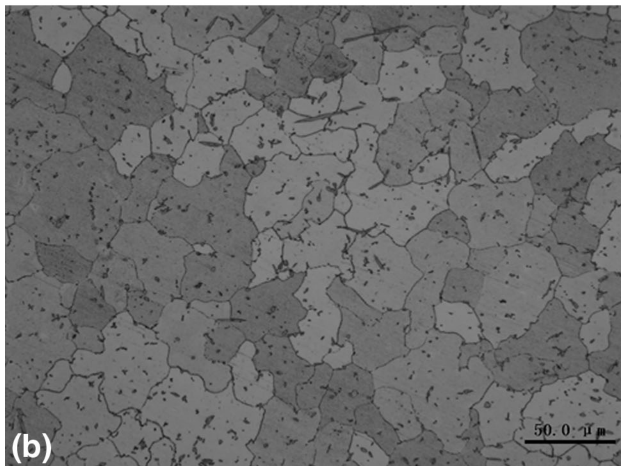

Fig. 2 As-cast microstructures of Cu-3Ti-2Sn (a) and Cu-2Ti-2Sn alloys (b)

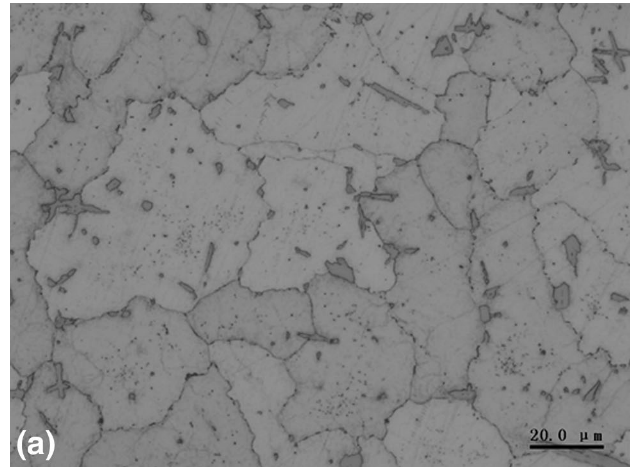

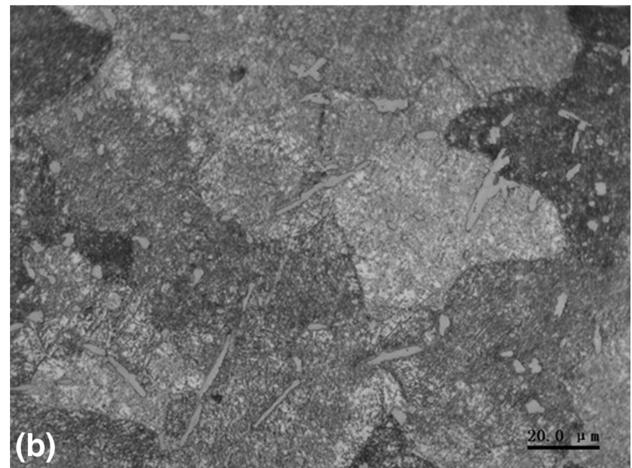

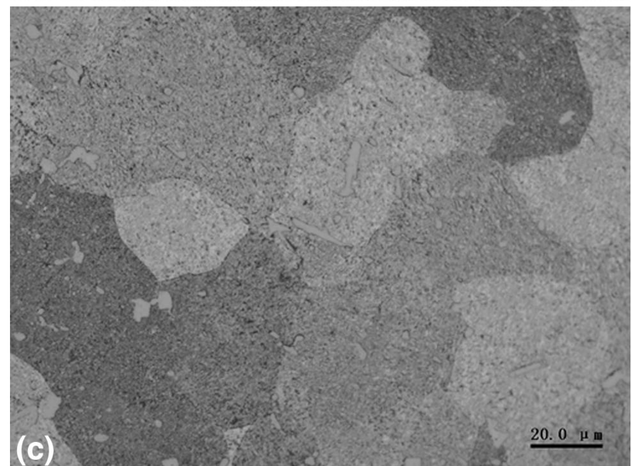

Fig. 3 Microstructures of Cu-3Ti-2Sn aged at 450 °C for 1 h (a), 4 h (b), and 8 h (c)

TUKON2100 microhardness tester at the load of 50 g holding for 15 s. The measured value is the average of five readings taken for each measurement. Light optical metallographic analysis was done on mechanically polished and etched samples. The etchant used was a mixture of 5 g $FeCl_3$, 15 mL HCl, and 100 mL distilled water. The microstructures were examined in a GX71 optical microscope. The specimens for TEM observation were cut from the aged samples using a Buehler's Isomet low-speed saw and then mechanically polished to obtain the slices with a thickness of 50 μm. Disks of 3 mm diameter were punched out from the slices, followed by thinning in an M691 ion milling at 4.5 kV. The thin foils were examined by a JEM-2100 transmission electron microscope (TEM) operated at 120 kV.

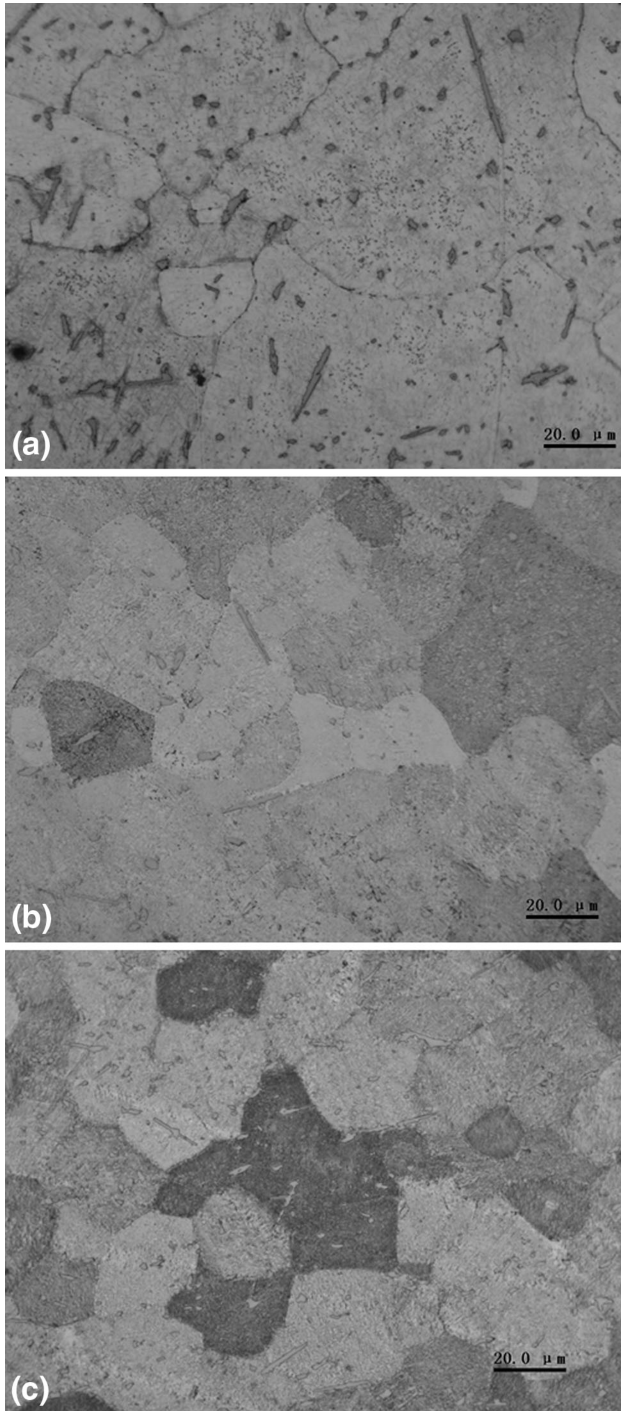

Fig. 4 Microstructures of Cu-2Ti-2Sn aged at 450 °C for 1 h (a), 4 h (b), and 8 h (c)

3. Results and Discussion

3.1 Microstructures and Properties of the As-cast Cu-Ti-Sn Alloys

Figure 1 shows the XRD pattern of the as-cast Cu-3Ti-2Sn alloy. It is learnt that the secondary phase is $CuSn_3Ti_5$

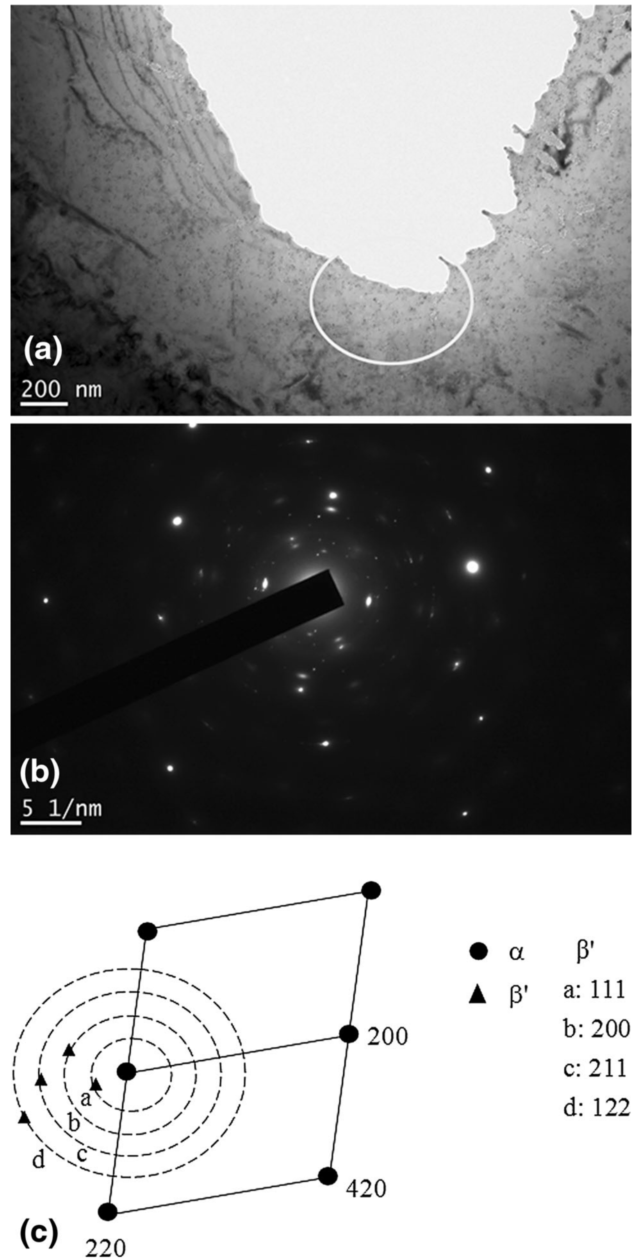

Fig. 5 TEM images of Cu-3Ti-2Sn alloy after aging at 450 °C for 1 h. (a) BF image, (b) SAD, and (c) Schematic of SAD pattern

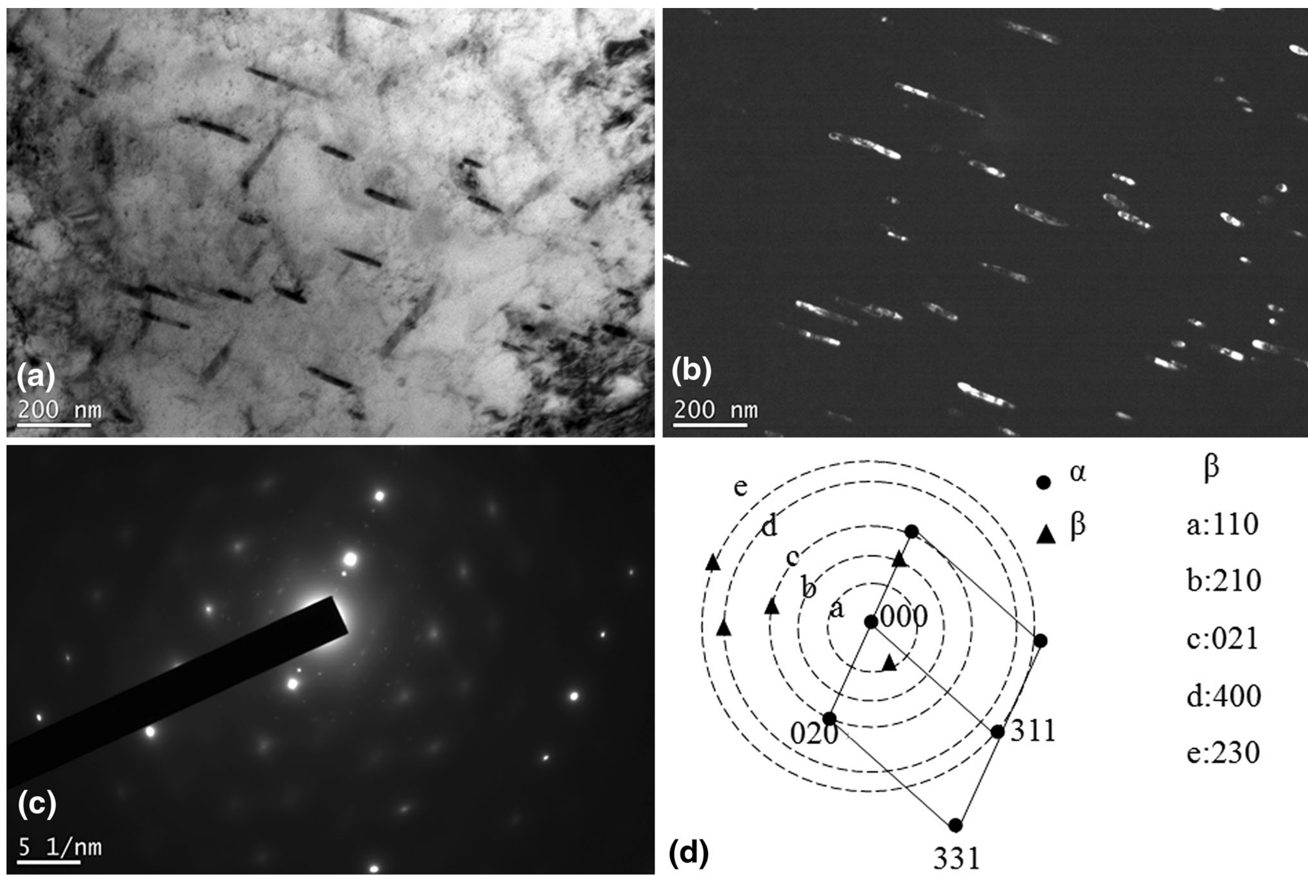

Fig. 6 TEM images of Cu-2Ti-2Sn alloy aged at 450 °C for 4 h. (a) BF, (b) DF, (c) SAD, and (d) Schematic of SAD

intermetallic compound. It is interesting to notice that the phase is different from the result reported by Lebreton et al. (Ref 14). They thought that the secondary phase is in the presence of the ternary eutectic intermetallic $CuTi_3Sn_5$ in the as-cast state. This is probably caused by the different Sn content. The microstructures of the as-cast Cu-3Ti-2Sn and Cu-2Ti-2Sn alloys are shown in Fig. 2(a) and (b), respectively. As seen from Fig. 2, $CuSn_3Ti_5$ phase distributes inside the copper grain and at the grain boundary in the as-cast ternary Cu-Ti-Sn alloys. The average grain size of Cu-3Ti-2Sn measured utilizing the linear intercept method is 37 μm, which is less than that of Cu-2Ti-2Sn alloy (50 μm). The measured electrical conductivity and hardness value of the as-cast Cu-3Ti-2Sn alloy are 4.4 MS/m and 98.6 HV, respectively, while Cu-2Ti-2Sn alloy has the electrical conductivity of 7.8 MS/m and the hardness value of 93.2 HV. It suggests that more Ti content is favorable for the improvement on the hardness, but deteriorates the electrical conductivity of the as-cast Cu-Ti-Sn alloys.

3.2 Microstructural Evolution of the Aged Cu-3Ti-2Sn and Cu-2Ti-2Sn Alloys

Figure 3 and 4 show the microstructures of Cu-3Ti-2Sn and Cu-2Ti-2Sn alloys after various aging times, respectively. As seen from Fig. 3(a) and 4(a), a small amount of fine precipitates form in the copper matrix after aging at 450 °C for 1 h. It is also noticed that there are still some residues of $CuSn_3Ti_5$ intermetallic compound even after solution treatment. With the increase of aging time, larger numbers of the precipitates present in the copper matrix and at grain boundaries, see Fig. 3 (b) and 4(b). At 8 h, fine precipitates are uniformly distributed in the copper matrix and at grain boundaries, as shown in Fig. 3 (c) and 4(c).

3.3 TEM Characterization

To understand the precipitation behavior of Cu-Ti-Sn alloy during aging process, TEM analysis was performed on the aged Cu-3Ti-2Sn and Cu-2Ti-2Sn alloys. Figure 5(a) to (c) shows the bright-field image (BF), the selected area diffraction (SAD) pattern, and its schematic diagram for Cu-3Ti-2Sn alloy aged at 450 °C for 1 h, respectively. A number of nano-sized particle precipitates can be observed in the copper matrix, as shown in Fig. 5(a). It can be identified from Fig. 5(b) and (c) that the fine precipitates are β′-Cu_4Ti phase, which has a body-centered tetragonal crystal structure with lattice parameters $a = 0.4530$ nm and $c = 1.2930$ nm. The precipitation of the fine, coherent, metastable β′-Cu_4Ti phase plays a predominant role in age hardening of Cu-Ti alloys (Ref 2).

TEM observation was also performed on the Cu-2Ti-2Sn alloy aged at 450 °C for 4 h. Figure 6(a) to (d) shows the bright-field image (BF), dark-field image (DF), selected area diffraction (SAD) pattern, and its schematic diagram, respectively. It can be seen from Fig. 6(a) and (b) that a number of vermicular secondary particles ranging from 20 to 150 nm precipitate discontinuously in the copper matrix. It is demonstrated from Fig. 6(c) and (d) that the fine precipitates are β-Cu_3Ti phase, which belongs to orthorhombic crystal structure with the lattice parameters $a = 0.5162$ nm, $b = 0.4347$ nm, and $c = 0.4531$ nm. The finding is in agreement with the literatures

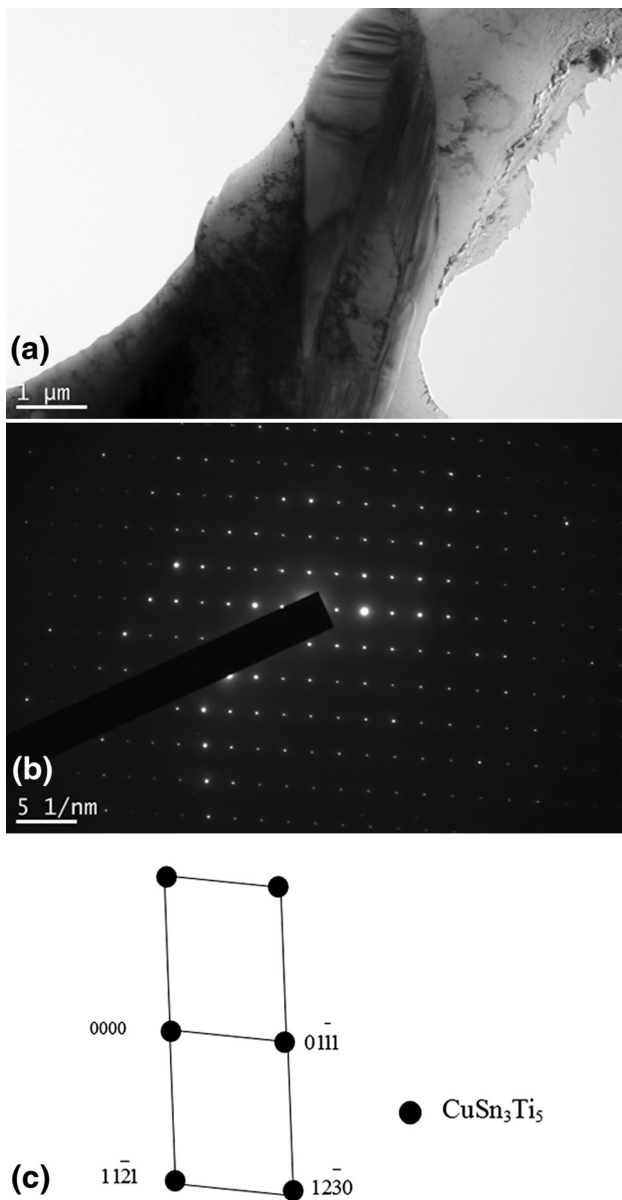

Fig. 7 TEM images of particle in the Cu-2Ti-2Sn alloy aged at 450 °C for 4 h. (a) BF, (b) SAD, and (c) Schematic of SAD

reported by Nagarjuna et al. (Ref 2) and Markandeya et al. (Ref 10, 13). They thought that the coherent metastable β′-Cu_4Ti phase precipitates at the early stage of aging for Cu-Ti alloys, but the prolonged aging time gives rise to the formation of incoherent equilibrium β-Cu_3Ti phase.

In the aged Cu-2Ti-2Sn alloy, it can also be seen that there is a small amount of large particles. Figure 7(a) to (c) shows the bright-field image of Cu-2Ti-2Sn alloy aged at 450 °C for 4 h, selected area diffraction (SAD) pattern, and its schematic diagram, respectively. It can be seen that there is the presence of an undissolved particle, see Fig. 7(a). From Fig. 7(b) and (c), it can be further demonstrated that the particle is in $CuSn_3Ti_5$ phase having a hexagonal structure with the lattice parameters $a = 0.8174$ nm, $b = 0.8174$ nm, and $c = 0.5577$ nm. This is in good accordance with the result of XRD. Hence, the ternary Sn element is existed as a $CuSn_3Ti_5$ intermetallic compound.

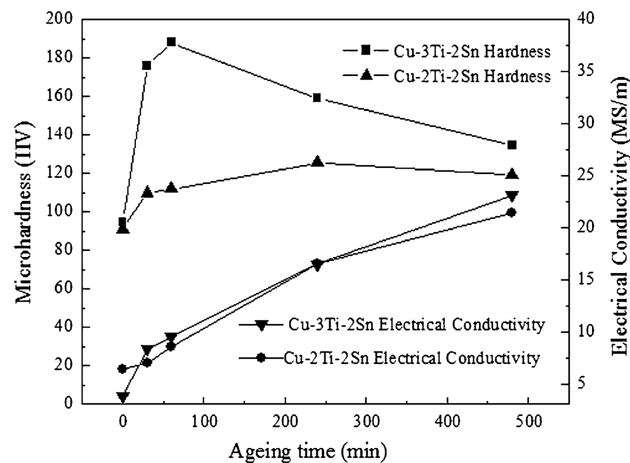

Fig. 8 The effect of aging time on the electrical conductivity and hardness of Cu-Ti and Cu-Ti-Sn alloys

3.4 The Electrical Conductivity and Hardness of the Aged Cu-3Ti-2Sn and Cu-2Ti-2Sn Alloys

The effect of aging time on the electrical conductivity of aged Cu-3Ti-2Sn and Cu-2Ti-2Sn alloys is presented in Fig. 8. For both Cu-3Ti-2Sn and Cu-2Ti-2Sn alloys, the electrical conductivity is significantly improved with the increase of aging time. The electrical conductivity of Cu-3Ti-2Sn alloy can reach 8.4 MS/m after aging at 450 °C for 0.5 h. After aging at 450 °C for 1 h, the electrical conductivity has a slight increase for both Cu-3Ti-2Sn and Cu-2Ti-2Sn alloys. After aging at 450 °C for 4 h, the electrical conductivity of Cu-3Ti-2Sn is quite close to that of Cu-2Ti-2Sn alloy. At 8 h, the electrical conductivity of Cu-3Ti-2Sn and Cu-2Ti-2Sn alloys reaches up to 23.1 and 21.5 MS/m, respectively. This can be explained as follows. Although the electrical conductivity is sensitive to a number of microstructural factors including vacancy concentration, solute concentration in the matrix, precipitate size, and precipitate volume fraction, the electrical conductivity primarily depends on the solubility of alloying elements in the matrix (Ref 15–17). At the initial stage of secondary aging, large supersaturated concentrations of Ti and Sn solute atoms in the Cu matrix affect the precipitation kinetics behavior and increase the formation rates of precipitates. Eventually, these solute atoms in the Cu matrix are greatly reduced by the precipitation of the second phases during aging, which decrease lattice distortion and electron scattering remarkably, giving rise to the increase of the electrical conductivity. However, the concentrations of Ti and Sn elements in the Cu matrix reduce progressively with further aging and the amount of precipitates decrease correspondingly. Hence, a slow increment occurs in the electrical conductivity after aging for 4 h.

As seen from Fig. 8, it is evident that the hardness increases and then decreases with the increase of aging time for both the alloys. At 0.5 h, the hardness of Cu-3Ti-2Sn alloy is 176 HV, which is increased by 66% in comparison with that of Cu-2Ti-2Sn alloy (110 HV). After aging for 1 h, Cu-3Ti-2Sn alloy reaches its peak hardness (188 HV), then the hardness of Cu-3Ti-2Sn alloy decreases progressively. Nevertheless, Cu-2Ti-2Sn alloy reaches its peak hardness of 125.5 HV after aging for 4 h. This change is closely related to the formation of

precipitated phases and phase transformation. Since higher Ti content for Cu-3Ti-2Sn alloy affects the precipitation kinetics and increases the precipitation rate, β′-Cu_4Ti phase precipitates from supersaturate Cu matrix more quickly at the early stage of aging in comparison with that of Cu-2Ti-2Sn alloy. Moreover, β′-Cu_4Ti phase is coherent with the Cu matrix (Ref 18). Thus, Cu-3Ti-2Sn alloy can reach its peak hardness value earlier than Cu-2Ti-2Sn alloy. However, further aging gives rise to the phase transformation from β′-Cu_4Ti to incoherent equilibrium Cu_3Ti (Ref 19) and the precipitate coarsening which does not act as an effective barrier against the dislocation motion, thus resulting in the decrease of the hardness.

4. Conclusions

1. The as-cast microstructure of Cu-Ti-Sn alloy consists of α-Cu(Ti,Sn) and primary $CuSn_3Ti_5$ intermetallic compound. $CuSn_3Ti_5$ phase has a hexagonal structure with the lattice parameters $a = 0.81737$ nm, $b = 0.81737$ nm, and $c = 0.55773$ nm.
2. With the increase of aging time, the hardness increases and then decreases, while the electrical conductivity progressively increases. In the range of experiments, the optimum aging process which can achieve good comprehensive properties is at 450 °C for 8 h. The electrical conductivity and hardness of Cu-3Ti-2Sn alloy are 23.1 MS/m and 134.5 HV, respectively, and those of Cu-2Ti-2Sn alloy are 21.5 MS/m and 119.3 HV, respectively.
3. The presence of $CuSn_3Ti_5$ phase reduces the solute Ti content in the copper, giving rise to the increase of the electrical conductivity for Cu-Ti-Sn alloys.
4. Both Cu-3Ti-2Sn and Cu-2Ti-2Sn alloys can be hardened by the precipitation of metastable and coherent β′-Cu_4Ti phase. The decrease of hardness after prolonged aging time is due to the formation of incoherent equilibrium β-Cu_3Ti phase and the coarsening of precipitates.

Acknowledgments

This research was supported by the National Natural Science Foundation of China (Nos. 51201132 and 51274163), the Research Program of Shaanxi Provincial Key Laboratory (13JS076), the China Scholarship Council, and Shaanxi Provincial Project of Special Foundation of Key Disciplines (2011HBSZS009).

References

1. W.A. Soffa and D.E. Laughlin, High-Strength Age Hardening Copper-Titanium Alloys, *Prog. Mater. Sci.*, 2004, **49**(3–4), p 347–366
2. S. Nagarjuna, M. Srinivas, K. Balasubramanian, and D.S. Sarma, On the Variation of Mechanical Properties with Solute Content in Cu-Ti Alloys, *Mater. Sci. Eng. A.*, 1999, **259**(1), p 34–42
3. C. Borchers, Catastrophic Nucleation During Decomposition of Cu-0.9at.%Ti, *Phil. Magi. A.*, 1999, **79**(3), p 537–547
4. P. Liu, F.Z. Ren, and S. G. Jia, 铜合金及其应用 (*Copper Alloys and Applications*), 1st ed., Chemical Industry Press, Beijing, 2007, p 110-112 [in Chinese]
5. D. Bozic, M. Mitkov, and M.T. Jovanovi, Structure and Microhardness of Precipitation/Dispersion Hardened Cu-Ti-B and Cu-Ti-Si Alloys, *Mater. Charact.*, 1994, **32**, p 97–103
6. S. Nagarjuna, K. Balasubramanian, and D.S. Sarma, Effect of Ti Additions on the Electrical Resistivity of Copper, *Mater. Sci. Eng. A.*, 1997, **225**(1–2), p 118–124
7. S. Nagarjuna, M. Srinivas, K. Balasubramanian, and D.S. Sarma, On the Deformation Characteristics of Solution Treated Cu-Ti Alloy, *Scripta Metal. Mater.*, 1995, **33**(9), p 1455–1460
8. S. Suzuki, K. Hirabayashi, H. Shibata, K. Mimural, M. Isshiki, and Y. Waseda, Electrical and Thermal Conductivities in Quenched and Aged High-Purity Cu-Ti Alloys, *Scripta Mater.*, 2003, **48**(4), p 431–435
9. R. Markandeya, S. Nagarjuna, and D.S. Sarma, Effect of Prior Cold Work on Age Hardening of Cu-4Ti-1Cr Alloy, *Mater. Charact.*, 2005, **404**(1–2), p 305–313
10. R. Markandeya, S. Nagarjuna, and D.S. Sarma, Precipitation Hardening of Cu-Ti-Cr Alloys, *Mater. Sci. Eng. A.*, 2004, **371**(1–2), p 291–305
11. S. Semboshi, T. Al-Kassab, R. Gemma, and R. Kirchheim, Microstructural Evolution of Cu-1at.%Ti Alloy Aged in a Hydrogen Atmosphere and Its Relation with the Electrical Conductivity, *Ultramicroscopy*, 2009, **109**(5), p 593–598
12. T.J. Konno, R. Nishio, S. Semboshi, T. Obsuna, and E. Okunishi, Ageing Behavior of Cu-Ti-Al Alloy Observed by Transmission Electron Microscopy, *J. Mater. Sci.*, 2008, **43**, p 3761–3768
13. R. Markandeya, S. Nagarjuna, and D.S. Sarma, Precipitation Hardening of Cu-3Ti-1Cd Alloys, *J. Mater. Eng. Perform.*, 2007, **16**(5), p 640–646
14. V. Lebreton, D. Pachoutinski, and Y. Bienvenu, An Investigation of Microstructure and Mechanical Properties in Cu-Ti-Sn Alloys Rich in Copper, *Mater. Sci. Eng. A.*, 2009, **508**, p 83–92
15. B. Raeisiula and W.J. Poole, Electrical Resistivity Measurements: A Sensitive Tool for Studying Aluminum Alloys, *Mater. Sci. Forum*, 2006, **519–521**, p 1391–1396
16. F.A. Guo, C.J. Xiang, C.X. Yang, X.M. Cao, S.G. Mu, and Y.Q. Tang, Study of Rare Earth Elements on the Physical and Mechanical Properties of a Cu-Fe-P-Cr Alloy, *Mater. Sci. Eng. B.*, 2008, **147**(1), p 1–6
17. Y. Feng, R.C. Wang, and C.Q. Peng, Influence of Ageing Treatments on Microstructure and Electrochemical Properties in Mg-8.8Hg-8Ga Alloy, *Intermetallics*, 2013, **33**, p 120–125
18. R. Markandeya, S. Nagarjuna, D.V.V. Satyanarayana, and D.S. Sarma, Correlation of Structure and Flow Behavior of Cu-Ti-Cd Alloys, *Mater. Sci. Eng. A.*, 2005, **428**(1–2), p 233–243
19. R. Markandeya, S. Nagarjuna, and D.S. Sarma, Effect of Prior Cold Work on Age Hardening of Cu-3Ti-1Cr Alloy, *Mater. Charact.*, 2006, **57**(4–5), p 348–357